THE FRICTIONAL PROPERTIES OF JOINTS IN ROCK

by J. C. JAEGER (*)

Summary — The conditions for sliding over artificial joint surfaces have been studied experimentally by cutting rock cylinders at various angles to their axes and studying slip over these surfaces in a triaxial testing apparatus. The types of joint used were: (i) filled with plaster to simulate a soft joint filling, (ii) bare surfaces ground approximately flat, and (iii) natural surfaces across which shear failure had taken place. The results agreed reasonably well with the simple theory for a constant coefficient of friction. Measured coefficients of friction lie in the range 0.5-0.8 and differ by surprisingly little between the various surfaces. The surfaces across which sliding has taken place exhibit interesting slickenside phenomena. Subsidiary failures frequently occur which cut across the joint surfaces.

1. *Introduction* — The study of the sliding of two approximately plane rock surfaces across one another is of the greatest importance in rock mechanics. The assumption usually made is the linear one, namely that, if N is the normal stress across the surface and τ the magnitude of the shear stress across it, slip can not take place if

$$\tau < \mu N + S_0 , \tag{1}$$

where μ is the coefficient of friction, assumed constant, and S_0 is a constant added to represent the shear strength or « cohesion » of the material filling the joint.

Because of the variable nature of the surfaces and rock materials there is little point in making assumptions which are more elaborate mathematically than (1) and this relation has been used extensively for studying the behaviour of jointed rock systems, mostly on a large scale, cf. TALOBRE [1]. The present work consists of a laboratory investigation intended to see how far the law (1) fits the experimental facts and to gain information about the coefficient of friction and the process of sliding between rock surfaces.

The apparatus used is virtually a copy of the small triaxial rig of the U.S. Bureau of Reclamation and is fully described by PATERSON [2]. In it, a rock cylinder of length 12.5 cm and diameter 5.08 cm can be subjected to an axial stress applied by a testing machine in addition to confining pressures of up to 1000 bars applied to its surface by oil pressure. The specimen is surrounded by a rubber

(*) Professor of Geophysics, Australian National University, *Canberra*.

jacket to prevent it from coming into contact with the oil. The cylinder rests with its lower end on a spherical seat, and for large displacements rotation of this seat may introduce interesting and important subsidiary effects which are discussed in § 6.

To provide model joints, cylinders were cut by a diamond saw across planes inclined at angles α to their axes running at 5° intervals between 25° and 65°. The lower limit of 25° was set by the geometry of the system (unfortunately, since smaller values of α are interesting theoretically) while for angles $\alpha > 65°$ failure took place through the rock, ignoring the joint.

The joints used were: (i) « Plaster », consisting of a layer of commercial patching plaster about 1 mm thick, (ii) « Bare surfaces », in which the two sides of a diamond saw cut, lightly ground and flat to better than 0.05 mm, were in direct contact, (iii) « Natural shear surfaces », consisting of reasonably flat surfaces across which cylinders of the solid rock had failed in shear.

Each of these types has its own characteristics: they are discussed in §§ 3, 4, 5, respectively. In all cases it is found that the result (1) holds approximately but not accurately: firstly there is usually a slight curvature of the τ, N curve, and, secondly, slip seems to be possible at higher values of α than would be expected from observations at low values. The interesting result emerges that the variation in the coefficient of friction between the various types of surface is not large, all the values measured lying in the range 0.40-0.86.

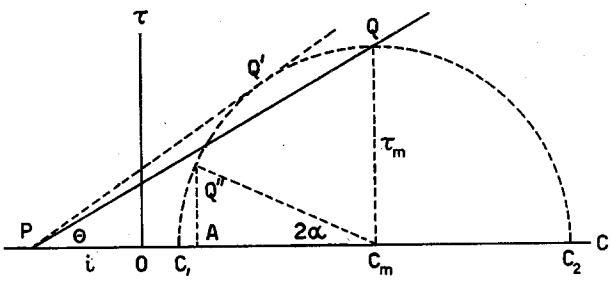

Fig. 1

Because of scatter of the experimental points and curvature of the τ, N curves it is impossible to give values for the cohesion S_0 in (1). Usually, at least for low values of the mean stress, it is small.

2. *Theory* — It is sufficient to consider two-dimensional theory in the plane through the axis of the cylinder and perpendicular to the joint plane. If C_1 and C_2, $C_1 > C_2$, are the principal stresses in this plane, compression being reckoned positive, the normal stress N and the magnitude τ of the shear stress across a plane inclined at α to the direction of C_1 are given by [cf. JAEGER (3), § 3]

$$N = C_m - \tau_m \cos 2\alpha , \tag{2}$$

$$\tau = \tau_m \sin 2\alpha , \tag{3}$$

where

$$\tau_m = \tfrac{1}{2}(C_1 - C_2) \tag{4}$$

is the maximum shear stress, and

$$C_m = \tfrac{1}{2}(C_1 + C_2) \tag{5}$$

is the mean of the principal stresses. Using these results and writing

$$\mu = \tan \varphi\,, \tag{6}$$

where φ is the angle of friction, the criterion (1) for no slip becomes

$$\tau_m \sin(2\alpha + \varphi) < C_m \sin \varphi + S_0 \cos \varphi\,. \tag{7}$$

Plotted in the C, τ plane the values of τ_m and C_m for which failure takes place will lie on a « fracture curve » which is the straight line PQ of Fig. 1 whose inclination θ to the C-axis is

$$\tan \theta = \frac{\sin \varphi}{\sin(2\alpha + \varphi)}\,, \tag{8}$$

and whose intercept i on the C-axis is

$$i = -S_0 \cot \varphi\,. \tag{9}$$

The variation of the inclination θ of the fracture curve with α for various values of φ is shown in Fig. 2. If $\alpha = \frac{1}{2}\pi - \varphi$, $\theta = \pi/4$ and $C_2 \leq 0$. Thus $0 < \alpha < \frac{1}{2}\pi - \varphi$ is approximately the range of α in which slip is possible with both principal stresses compressive. When $\alpha = (\pi/4) - \frac{1}{2}\varphi$, the curves of Fig. 2 have

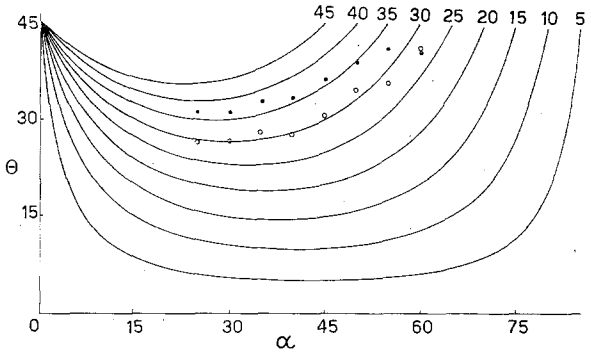

Fig. 2 - *Variation of the inclination* θ *of the fracture curve with* α *for various values of* φ. The numbers on the curves are the values of φ. Dots: experimental points for plaster joints. Circles: experimental points for bare joints.

a minimum so that this value gives most favourable direction of slip. Further, this minimum is rather flat, particularly for the smaller values of φ: this implies that the stress-difference necessary to cause slip varies slowly near the most favourable direction but more rapidly as $\alpha \to 0$ or $\alpha \to \frac{1}{2}\pi - \varphi$.

The plot of τ_m against C_m in Fig. 1 is one of the many representations of the criterion for failure: it has been chosen because of its relationship to the Mohr theory. By (1) the normal and shear stresses across the plane included at α to C_1 are given by OA and AQ'' in Fig. 1, respectively. A Mohr envelope PQ' can be

drawn in the usual way which passes through P and makes an angle θ_m with the C-axis given by

$$\sin \theta_m = \tan \theta \,. \tag{10}$$

This Mohr envelope has no significance in the present case since the points Q'' corresponding to failure are seen from Fig. 1 always to lie inside it except in the special case

$$\alpha = (\pi/4) - \tfrac{1}{2}\varphi \quad \text{for which} \quad 2\alpha = \tfrac{1}{2}\pi - \theta_m = \tfrac{1}{2}\pi - \varphi \,.$$

In experiments of the present type, in which a joint at a definite angle α is filled with solid material and stressed, there are three separate effects, all described to a linear approximation by the same mathematics with their own appropriate constants. These are: (i) shear failure of the joint material, in this case S_0 will be the shear strength of the filling material and μ its coefficient of internal friction;

(ii) sliding of the sheared material along the plane, here μ is a coefficient of friction in the ordinary sense and S_0 represents the « cohesion » of the sheared material;

(iii) at unfavourable angles of the joint, the material of the cylinder may fail leaving the joint intact, in this case $\mu = \tan \varphi$ is the coefficient of internal friction of the material of the cylinder and shear failure of this material takes place at the Coulomb-Navier angle of $(\pi/4) - \tfrac{1}{2}\varphi$.

3. *Plaster Joints* — In order to simulate a joint filled with solid material a layer of commercial patching plaster about 1 mm thick was used. The plaster joints were dried in air for a week before testing. Angles α at 5° intervals between 25° and 65° were used. If $\alpha > 60°$ failure usually took place through the material of the cylinder, ignoring the joint; this is consistent with the angles of friction of between 25° and 30° found below.

Cylinders were all cut from the same material, a quartz porphyry of grain size of the order of 1-3 mm. A series of triaxial tests were made on this material and its C_m, τ_m curve for fracture is shown in Fig. 5.

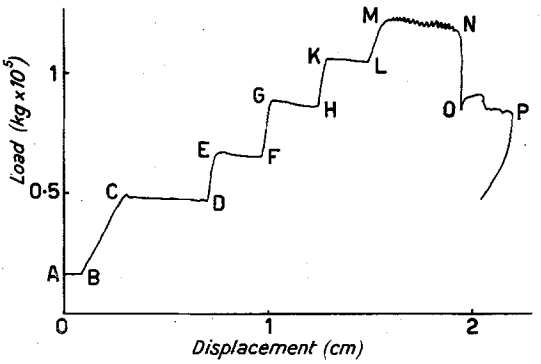

Fig. 3 - *Load-displacement curve for a plaster joint at* $\alpha = 50°$.

The method of testing and the type of results obtained may be illustrated by reference to Fig. 3 which is a load-displacement curve obtained from the recorder of the testing machine for the case $\alpha = 50°$. In all of Figs. 3, 6, 7 the load mea-

sured by the machine consists of the axial load on the specimen plus the load on the exposed parts of the piston (diameter 9.84 cm) due to the oil pressure.

In the test of Fig. 3 the confining pressure is first raised to 200 bars corresponding to AB; at B contact is made with the specimen, and BC corresponds to axial loading at a confining pressure of 200 bars; at C there is a definite slip in the material and this is taken as the point of shear failure of the joint material; the confining pressure is maintained at 200 bars and the region CD in which the load remains remarkably constant during a quite large displacement is traversed, corresponding to sliding over the joint surface; the confining pressure is raised to 400 bars at D, and EF corresponds to sliding at 400 bars; the process is repeated, and GH, KL and MN correspond to sliding at 600, 800 and 1000 bars, respectively. The region $MNOP$ will be discussed further in § 6.

The experiment of Fig. 3 was one of a number made to demonstrate the constancy of load in the regions CD, EF, etc. These large displacements are not desirable since they force the specimen further and further into the configuration of Fig. 8-a. In the experiments made for purposes of measurement, the regions CD, EF, ... were much shorter, also, in most cases, measurements were made at decreasing as well as increasing confining pressures. The difference between the two sets of values was usually only a few percent. Because of the rather crude nature of the experiments no correction for friction of the piston was made; this was shown by PATERSON [2] to be of the order of 3 percent of the total load.

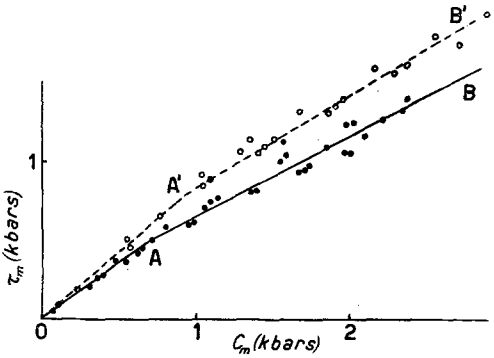

Fig. 4 - *Variation of maximum shear stress* τ_m *with mean principal stress* C_m *for sliding on a plaster joint.* Circles for $\alpha = 55°$, dots for $\alpha = 45°$.

In all cases the experimental values were plotted on a C_m, τ_m diagram for comparison with the theory of § 2. To show the consistency of the experimental results actual values for $\alpha = 45°$ (dots) and $\alpha = 55°$ (circles) are shown in Fig. 4. The scatter in *individual* runs is much smaller, this is probably attributable both to variation in thickness and ageing of different plaster joints and to the fact that joint material which is broken at higher confining pressures probably behaves differently (because it has been greatly compressed) to that broken at the low pressures. Both the individual curves and the composite results of Fig. 4 suggest that the C_m, τ_m curve is not a straight line but shows slight curvature. This curvature, as well as the scatter of the individual points, diminishes as α diminishes. The

results of Fig. 4 can be represented roughly by two straight lines OA and OA' leading to initial values μ_i of the coefficient of friction, and two straight lines AB, $A'B'$ of lesser slope leading to final values μ_f of the coefficient of friction. The results of the experiments at all other values of α were treated in the same way and coefficients of friction μ_i and μ_f deduced from (8). These results are shown in the first two columns of Table 1.

TABLE 1 - *Variation of coefficient of friction with* α : μ_i *from initial part of curve,* μ_f *from final part.* μ' *is the coefficient of internal friction of the joint material.*

α	μ_i	μ_f	μ'
60°	0.52	0.40	0.50
55°	0.63	0.44	0.57
50°	0.69	0.53	0.50
45°	0.73	0.52	0.62
40°	0.72	0.56	0.62
35°	0.78	0.57	0.58
30°	0.74	0.56	0.65
25°	0.74	0.61	

If the linear theory of § 2 held exactly, μ_i in Table 1 should be equal to μ_f and independent of α. The variation shows the measure of the inapplicability of the theory. As an alternative representation, experimental values of θ corresponding to μ_i for various values of α are shown by dots in Fig. 2. For $25° \leqq \leqq \alpha \leqq 50°$ these are reasonably consistent with the curve for $\varphi = 35°$, but for the highest values of α, 55° and 60°, for which slip would not be possible with the above value of φ, they fall too low. It should be remarked that experimental scatter is much greater at these high angles. For $\alpha = 60°$ the angle of friction is 27°, and this suggests that slip is impossible if $\alpha > 63°$ and in fact for $\alpha > 60°$ failure is usually observed through the material of the cylinder, ignoring the joint.

It is of some interest to study the conditions for failure of the joint material (point C in Fig. 3) at various confining pressures. As remarked in § 2 these may be interpreted by the same theory, leading to a coefficient of internal friction μ' for the joint-filling material. The variation of μ' with α is shown in the third column of Table 1. The fact that $\mu' < \mu_i$ is due to the finite shear strength of the joint material, while the early portions of the C_m, τ_m curves for sliding, from which μ_i has been calculated, appear to pass through the origin, cf. Fig. 5.

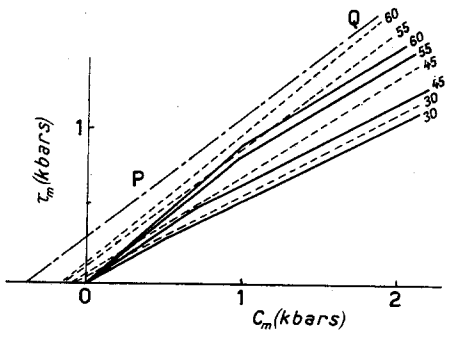

Fig. 5 - *Dotted lines: variation of* τ_m *with* C_m *for failure of plaster joints at* α = 60°, 55°, 45° *and* 30°. Full lines show the corresponding variation of sliding over broken joints. PQ is the C_m, τ_m curve for failure of the rock of the cylinder.

To show the relationship between the various results, the C_m, τ_m curves for sliding, obtained as in Fig. 4, for α equal to 60° 55°, 45° and 30° are shown by full lines in Fig. 5. Straight line approximations for failure of the joint material for the same values of α are shown by the dotted lines and are seen to lie a little above the corresponding curves for slip. Finally the C_m, τ_m curve for failure of the rock material of the cylinders is shown by *PQ*.

4. *Bare flat surfaces* — These consisted of two sides of a diamond saw cut, slightly ground with fine abrasive and placed together. The two surfaces were flat to within about 0.05 mm.

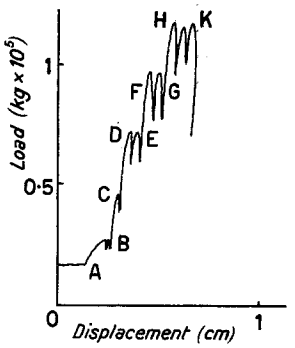

Fig. 6 - *Load-displacement curve for sliding over bare surfaces at* $\alpha = 25°$.

A typical load-displacement curve is shown in Fig. 6 for $\alpha = 25°$. It is quite different from those of Figs. 3 and 7. The region *AB* corresponds to loading under a confining pressure of 200 bars. There is a short initial period of sliding during which intimate contact is established over almost the whole of the surfaces. When this has taken place, subsequent movement is by a violent stickslip process of large amplitude. When two such slips had taken place at *B* the confining pressure was raised to 400 bars and slip at *C* corresponds to this pressure. Similarly, the two slips at *DE* occurred at 600 bars, those at *FG* at 800 bars, and the three at *HK* at 1000 bars. It appears that the loads at which slip occurs are surprisingly reproducible.

On removal from the testing machine the surfaces of the specimens are found to be covered with very fine powder and the trace of each individual slip can be clearly seen. The process of sliding appears to involve the crushing of the leading edges of prominent crystals. Well defined striations of slickenside type frequently occur.

The values of the coefficients of friction, calculated as before, are shown in Table 2. The C_m, τ_m curves are more nearly linear than those of Fig. 4 and only one straight line, passing near the origin, has been used in their reduction.

TABLE II - *Coefficients of friction for sliding of bare rock surfaces.*

α	25°	30°	35°	40°	45°	50°	55°	60°
μ	0.56	0.59	0.61	0.57	0.59	0.61	0.53	0.52

The variation of θ with α is shown by circles in Fig. 2. It appears that the behaviour is reasonably consistent with an angle of friction of 30°, except for a falling off at the highest values of α.

When the specimens are removed from the machine and the surfaces separated, a strong and characteristic smell similar to that found near rock crushers and tunnel faces or, sometimes, after breaking rocks, is noticed. This odour persists for some time. It seems possible that it is caused by heating of the rock powder during slip. It is impossible to predict the temperatures which may be attained but the following simple argument shows that they may be quite high. In an experiment at 1000 bars and $\alpha = 45°$, slip took place when the shear stress across the plane reached a value of 1.2×10^9 dynes/cm^2. The distance of slip, measured from the surface markings, was about 1 mm so that the heat liberated was of the order of 2.9 cal/cm^2. The amount of crushed rock flour between the surfaces was 0.004 gm/cm^2 so that if the above amount of heat was liberated in this material and an equal quantity in the rock on either side its temperature would be raised to about 3000° C.

5. *Natural surfaces of shear failure* — In addition to experimenting with artificially filled joints and with bare plane surfaces an attempt was made to study the frictional properties of the naturally occurring surfaces provided by shear fractures.

The first experiments of this type were made on specimens of granitic gneiss of grain size 1-2 mm which had failed along single shear planes under compression at a confining pressure of 1000 bars. These fracture surfaces were far from plane, irregularities of the order of 2 mm being common. Nevertheless it was found, on subjecting them to the routine described above, that they showed a remarkably uniform behaviour, giving a reasonably linear fracture curve with coefficients of friction of the order of 0.7.

On removing the specimens, the higher portions of their surfaces were found to be marked with well developed slickensides, while the hollows were filled with loose, fine rock powder. Frequently the slickensides were curved. When they showed steps these almost invariably faced the direction of motion [cf. PATERSON (2)]. In many cases these steps were clearly formed by the plucking out of individual grains. Occasional small stick-slips occurred in the stress-strain curves, which presumably indicated the removal of major asperities.

While no experiments have been made with pore-water under pressure, an attempt was made to see what effect the presence of water might have by soaking the surfaces in water before the experiment. The effect was quite marked: the fracture curve usually showed considerable curvature so the (slightly lower) coefficients of friction shown in Table III serve only as an indication of order of magnitude. The effect on the appearance of the surfaces was even more marked: the loose rock powder was compacted into a dense mylonite mass and the surfaces were completely covered with well developed slickenside markings, often strongly curved about surface irregularities.

Other experiments of the same type were made on the porphry described earlier, a fine-grained sandstone (Hawkesbury) and marble (Wombeyan), except that unbroken cylinders of the material were now stressed to failure at a chosen confining pressure, displacement being continued until a steady stress was attained corresponding to sliding across this plane, and, subsequently, frictional measurements being made at higher confining pressures. An example of a load-displace-

ment curve of this type is shown in Fig. 7 in which *B* corresponds to failure of the specimen at 200 bars confining pressure, the region *CD* to slip at 200 bars, and *E*, *F*, *G*, *H*, respectively, to slip at 400, 600, 800 and 1000 bars confining pressure.

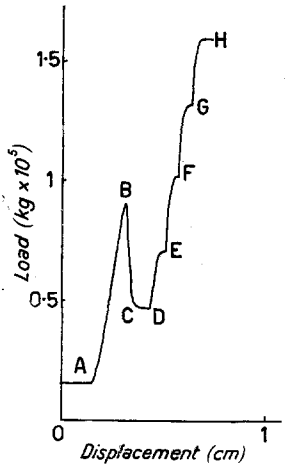

Fig. 7 - *Load-displacement curve for fracture of porphyry at 200 bars followed by sliding over the (approximately plane) fracture surface at various confining pressures.*

Using this method, the nature and angle of the fracture plane must be inferred from the final appearance of the specimen.

The behaviour of the different rocks varies, as might be expected, with their mechanical properties. The brittle porphyry showed a tendency to powder and to develop subsidiary shear fractures. The sandstone, which is capable of considerable plastic deformation at the higher confining pressures, showed remarkably plane fracture surfaces but had a tendency to overthrust along parallel planes [cfr. Fig. 8-e, 8-f]. The behaviour of the more plastic marble is also characteristic: if broken at a very low confining pressure such as 10 bars it merely shows sliding along a single slip plane; however if it is broken at a higher confining pressure of 100 bars, even if considerable displacements of the order of 2 mm along the slip plane are made at this pressure in the hope of establishing a single slip plane, the deformation appears to take place over a region which retains considerable strength, so that when, in this sequence of experiments, the confining pressure is raised, there is not only further slip over this plane but considerable plastic deformation of the usual type throughout the whole of the material.

TABLE. III - *Frictional properties of natural surfaces of failure.*

Material	α	μ (fracture)	μ (sliding)
Porphyry	25°	1.24	0.86
Marble	29°	0.67	0.62
Sandstone	33°	0.58	0.52
Sandstone (wet)	34°	0.73	0.47
Granitic gneiss	28°		0.71
Granitic gneiss (wet)	34°		0.61

The results of these experiments are shown in Table III. In each case several runs were made and the figures in the Table are those for the individual run nearest to the mean. Because of the rather crude nature of the experiments and curvature of the C_m, τ_m curves it is unsafe to give values of the cohesion, but in all cases it was small and usually much less than 200 bars. In those cases in which shear fractures were produced in the experiment the values of the coefficient of internal friction are also given. The relatively low values for sliding friction in sandstone are probably attributable to the very flat surfaces of shear fracture obtained with this material.

It should be remarked that the values of μ of the order of 0.62 obtained here for Wombeyan marble differ very considerably from the value of 2.4 given by PATERSON ([2]) for the same material. There are two reasons for this, firstly there was a numerical error in PATERSON's calculation and his values should range from 1.0 to 1.2, secondly his results were obtained from a single observation by neglecting S_0 in (1), so that $\mu = \tau/N$, and results obtained in this way must always be too large. In fact, as remarked above, marble, particularly at confining pressures of the order of 200 bars, shows a marked tendency to deform over a wide shear zone rather than a narrow region and this shear zone retains considerable shear strength of the order of 200 bars.

6. *Subsidiary failures* — In many cases at a late stage in the experiment when considerable displacement had taken place across the joint plane, subsidiary fractures of the cylinder took place. In some cases these occur as sudden failures with a considerable drop in load; in others, however, the only indication is that the loads measured with decreasing confining pressure were relatively low and in these cases a number of more or less definite planes of incipient fracture could be

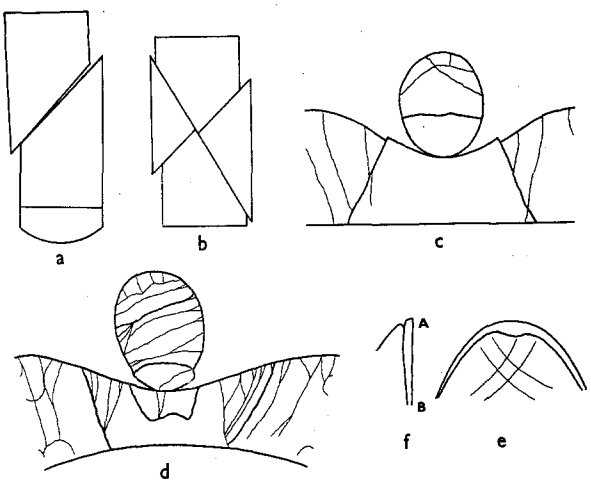

Fig. 8 - *Some typical fracture systems.* (a) *change of configuration caused by rotation of spherical seat:* (b) *typical fracture in the configuration of* (a): (c) *development of the surface fractures on a rock fractured as in* (b): (d) *development of surface fractures on a rock which has been almost completely crushed:* (e), (f) *surface development and elevation of overthrusting in sandstone during slip along AB.*

seen on removing the specimen; in some cases the specimens were almost completely crushed.

These subsidiary failures are usually caused by the change of the stress-system following the rotation of the spherical seat S into a configuration shown exaggerated in Fig. 8-a. They are believed to be of some interest since effects of these types must certainly occur in practical systems in which relative movement along a number of joint planes can take place.

Some examples will now be given. The material of the cylinders (porphyry) had an angle of internal friction of about 50°, giving an expected plane of shear failure at 20° to the axis of the cylinders. As remarked above, the configuration of the two halves of the specimen before fracture will be that of Fig. 8-a and the commonest form of fracture of the cylinders is along a plane inclined at about 20° to the axis and cutting across the joint plane as shown in Fig. 8-b. A development of the visible fractures on a specimen which has failed in this manner is shown in Fig. 8-c. In some cases shear failure takes place on both conjugate planes.

The load-displacement curve of Fig. 3 resulted in a failure at N of the type of Fig. 8-b. It was remarked that in that experiment the displacements were particularly large and in the region MN movement along the joint plane is by a series of small stick-slips: at N the stresses were sufficient to cause sudden shear failure of the material across the joint and the region OP corresponds to slip along this new surface. This observation may have some tectonic significance, namely that a series of small slips along one joint or fault plane may so change the pattern of stresses in a neighbouring block as to cause a major failure in it.

Fig. 8-d shows a development of the major fractures visible on the surface of a rock which has been greatly crushed. This specimen showed two distinct minor slips at a confining pressure of 1000 bars but was still supporting a stress-difference of 2800 bars. It is broken up by a series of nearly vertical fractures. The joint surface has become quite irregular and the rather plastic plaster has been forced into the cracks and surface irregularities.

It is a suggested that experiments of this type may be useful in determining the mechanical properties likely to be expected of the « destressed » rock common in deep mining practice. Also they may provide a useful method for determining the behaviour to be expected from different types of rock in crushers.

Finally, as an example of the types of geological behaviour which may be reproduced in this way, Fig. 8-e shows a surface development and Fig. 8-f an elevation of an overthrust produced during sliding of sandstone across a plane. Two major sets of slip lines, and many minor ones are strongly marked on the surface.

REFERENCES

(1) TALOBRE J.: *La mécanique des roches.* Dunod, Paris (1957). — (2) PATERSON M. S.: *Experimental deformation and faulting in Wombeyan marble.* Bull. Geol. Soc. America. Vol. 69, p. 465 (1957). — (3) JAEGER J. C.: *Elasticity, Fracture and Flow.* Methuen (1958).

(*Received on 24th March* 1959)